SANDIA REPORT

SAND97-0795 • UC-721
Unlimited Release
Printed August 1997

Final Disposal Room Structural Response Calculations

Charles M. Stone

Prepared by
Sandia National Laboratories
Albuquerque, New Mexico 87185 and Livermore, California 94550

Sandia is a multiprogram laboratory operated by Sandia Corporation, a Lockheed Martin Company, for the United States Department of Energy under Contract DE-AC04-94AL85000.

Approved for public release; distribution is unlimited.



SF2900Q(8-81)

Issued by Sandia National Laboratories, operated for the United States Department of Energy by Sandia Corporation.

NOTICE: This report was prepared as an account of work sponsored by an agency of the United States Government. Neither the United States Government nor any agency thereof, nor any of their employees, nor any of their contractors, subcontractors, or their employees, makes any warranty, express or implied, or assumes any legal liability or responsibility for the accuracy, completeness, or usefulness of any information, apparatus, product, or process disclosed, or represents that its use would not infringe privately owned rights. Reference herein to any specific commercial product, process, or service by trade name, trademark, manufacturer, or otherwise, does not necessarily constitute or imply its endorsement, recommendation, or favoring by the United States Government, any agency thereof or any of their contractors or subcontractors. The views and opinions expressed herein do not necessarily state or reflect those of the United States Government, any agency thereof or any of their contractors.

Printed in the United States of America. This report has been reproduced directly from the best available copy.

Available to DOE and DOE contractors from
Office of Scientific and Technical Information
PO Box 62
Oak Ridge, TN 37831

Prices available from (615) 576-8401, FTS 626-8401

Available to the public from
National Technical Information Service
US Department of Commerce
5285 Port Royal Rd
Springfield, VA 22161

NTIS price codes
Printed copy: A08
Microfiche copy: A01

SAND97-0795
Unlimited Release
Printed August 1997

Distribution
Category UC-721

Final Disposal Room Structural Response Calculations

Charles M. Stone
Engineering and Manufacturing Mechanics Department
Sandia National Laboratories
Albuquerque, NM 87185

Abstract

Finite element calculations have been performed to determine the structural response of waste-filled disposal rooms at the WIPP for a period of 10000 years after emplacement of the waste. The calculations were performed to generate the porosity surface data for the final set of compliance calculations. The most recent reference data for the stratigraphy, waste characterization, gas generation potential, and nonlinear material response have been brought together for this final set of calculations.

Acknowledgment

The author would like to acknowledge the contributions of J. Randall Weatherby and J. G. Arguello of Sandia National Laboratories who have been involved with the development of the disposal room model since the beginning. The author would like to also acknowledge the support and assistance of WIPP Principal Investigator B. M. Butcher.

Table of Contents

Acknowledgment 4
Table of Contents 5
List of Figures 6
List of Tables 7
Introduction 9
Disposal Room Model 11
Geomechanical Model 14
Stratigraphy and Numerical Model 14
Halite Constitutive Model 18
Waste Constitutive Model 21
Anhydrite Constitutive Model 21
Results of the Analyses 24
Summary of Results 29
References 30
Appendix A: 31
Appendix B: 35

List of Figures

Figure 1. A Typical Porosity Surface Used for the 1992 Comparison of Predicted WIPP Performance With 40 CFR Part 191, Subpart B (Butcher and Mendenhall, 1993). 10

Figure 2. History of the Reference Gas Generation Potential Used for the Disposal Room Analyses, f = 1.0. 12

Figure 3. Idealized Stratigraphy Near the Disposal Room Horizon Defined by Munson et al., 1989. 15

Figure 4. Simplified Statigraphic Model Used For the Current Disposal Room Analyses (Butcher, 1997). 16

Figure 5. Mesh Discretization and Boundary Conditions Used for the Disposal Room Analyses. 17

Figure 6. Curve of the Pressure-Bulk Strain Input to the Volumetric Plasticity Model Used to Model the Waste Drums 22

Figure 7. Pressure Histories for Various Values of the Gas Generation Parameter, f, for a Disposal Room Containing Waste Only. The Gas Generation Parameter Values Range From Bottom to Top: f = 0.025, 0.05, 0.10, 0.20, 0.40, 0.50, 0.60, 0.80, 1.0, 1.2, 1.6, and 2.0. 25

Figure 8. Porosity Histories for Various Values of the Gas Generation Parameter, f, for a Disposal Room Containing Waste Only. The Gas Generation Parameter Values Range From Bottom to Top: f = 0.0, 0.025, 0.05, 0.10, 0.20, 0.40, 0.50, 0.60, 0.80, 1.0, 1.2, 1.6, and 2.0. 25

Figure 9. Close-up View of the Deformed Disposal Room With Waste at 300 Years for f = 0.0. 27

Figure 10. Close-up View of the Deformed Disposal Room With Waste at 10,000 Years for f = 0.0. 27

Figure 11. Close-up View of the Deformed Disposal Room With Waste at 300 Years for f = 0.5. 28

Figure 12. Close-up View of the Deformed Disposal Room With Waste at 10,000 Years for f = 0.5. 28

List of Tables

Table 1. WIPP CH-TRU Waste Material Parameter Disposal Inventory (Butcher, 1997)11

Table 2. Salt Elastic Properties (Butcher, 1997) 20

Table 3. Salt Creep Properties (Butcher, 1997) 20

Table 4. Pressure-Volumetric Strain Data Used in the Volumetric-Plasticity Model for the Waste Drums (Butcher, 1997) 22

Table 5. Material Constants Used With the Volumetric Plasticity Model for the Waste (Butcher, 1997) 23

Table 6. Elastic and Drucker-Prager Constants for Anhydrite (Butcher, 1997) 23

Intentionally Left Blank

Introduction

The Waste Isolation Pilot Plant (WIPP) is a United States Department of Energy (DOE) research and development facility designed to demonstrate the safe management, storage, and long term disposal of both contact handled (CH-TRU) and remote handled (RH-TRU) transuranic waste generated by defense activities of the United States. The WIPP is located in southeastern New Mexico in bedded salt deposits at a depth of 655 m below the surface. Before the facility is allowed to accept waste for storage, the WIPP must be shown to be in compliance with the Environmental Protection Agency's (EPA) Standard *40 CFR Part 191* (EPA, 1985) and other regulations prescribing limits on the transport of radionuclide materials into the environment. Sandia National Laboratories is providing technical and scientific support to the DOE in demonstrating WIPP compliance with the regulations.

Compliance with the regulations will be established by performance assessment predictions of the long-term performance of the WIPP. Performance assessment means *an analysis that identifies the processes and events that might affect the disposal system, examines the effects of these processes and events on the performance of the disposal system, and estimates the cumulative releases of radionuclides, considering the associated uncertainties, caused by all significant processes and events* (Bertram-Howery et al., 1990). These long-term performance predictions are based on the results from mathematical models which provide the respository response. The overall repository model is composed of many smaller component models which describe various individual processes in detail, e.g. fluid flow, radionuclide transport, and sealing. The component model that is of interest in this report is the Disposal Room Model which provides information about the effects of room closure on the waste.

The performance assessment model requires estimates of the porosity of a waste-filled disposal room. Early performance assessment calculations assumed the porosity to be constant based on the waste composition. However, it became clear that realistic estimates of the porosity from a waste-filled, deforming room would be required. In addition, the effects of internal gas generation from decomposing waste would have to be included because the presence of the internally generated gas would greatly affect the closure of the disposal room. Realistic estimates of the change in disposal room porosity as a function of time require nonlinear finite element calculations which are expensive in both time and computer resources. The complete set of calculations, involving large numbers of analyses as required by the performance assessment methodology, made this approach totally unfeasible. Therefore, a simplified approach which effectively provided the necessary porosity data to the respository model was developed.

A less computationally intensive relationship between the amount of gas generation potential and room porosity was developed by constructing a simplified *porosity surface* from a minimal set of nonlinear finite element analyses. In each nonlinear analysis, a porosity time history curve was determined for a specific gas generation potential. The collection of porosity histories for various gas generation potentials were then combined to form the porosity surface shown in Figure 1. Interpolation on this surface could then be used by the repository model in the performance assessment calculation to correlate

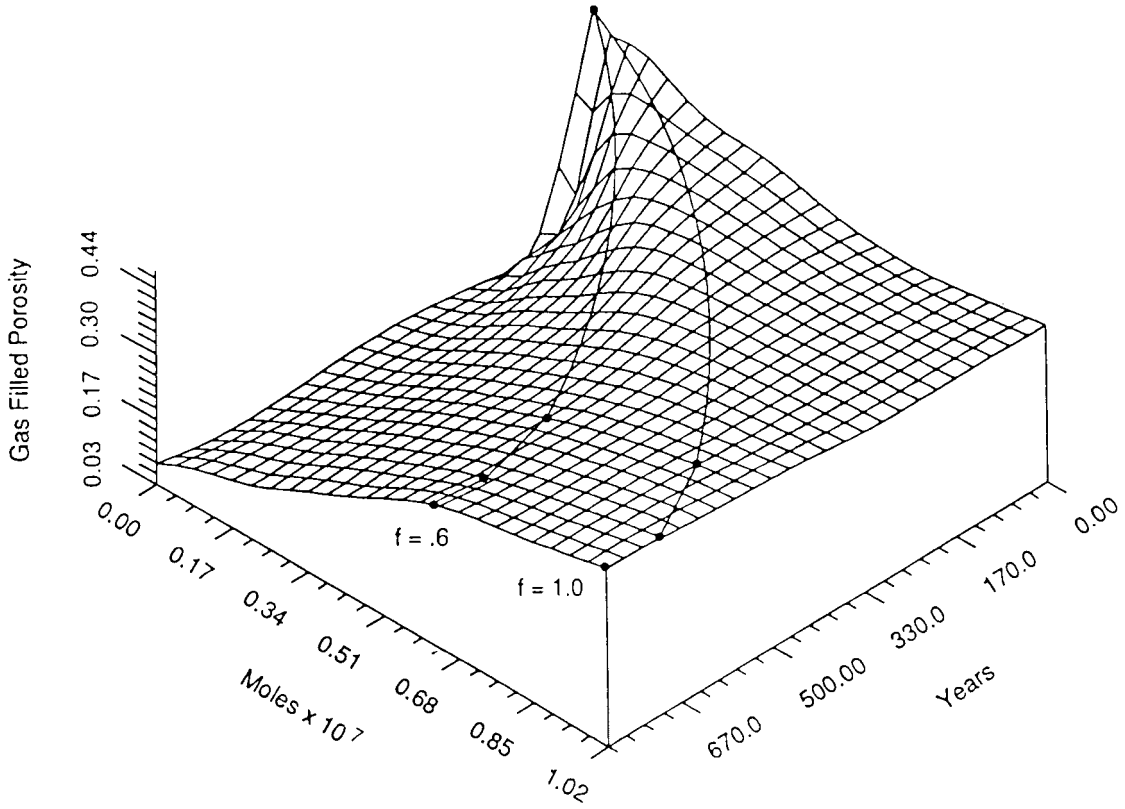


Figure 1. A Typical Porosity Surface Used for the 1992 Comparison of Predicted WIPP Performance With 40 CFR Part 191, Subpart B (Butcher and Mendenhall, 1993).

disposal room porosity with the amount of gas generation potential. This correlation is a simple matter of interpolation on the porosity surface.

This report documents the analyses performed to generate the porosity surface data for the final set of compliance calculations. This final set of calculations is based on presently accepted reference data for the stratigraphy, waste characterization, gas generation potential, and material response. The calculations were performed as described in "Analysis Plan: Final Porosity Surface Calculations, WBS 1.1.01.2.3, Rev 1, November 6,1995, WPO# 29792".

The next section of the report describes the disposal room model which includes information about the disposal room and the waste contents. The following section discusses the geomechanical model used for the analyses including descriptions of the idealized stratigraphy and the discretized finite element model. Also included in this section are descriptions of the constitutive models used in the analyses. References for the sources of all of the dimensions, values for constitutive model parameters, and other input information are given in (Butcher, 1997). The fourth section presents the results of the analyses and is followed by a summary of the results.

Disposal Room Model

The disposal plan for the WIPP calls for waste drums containing transuranic waste to be stored in long, rectangular shaped underground rooms mined in the bedded salt formations in southeastern New Mexico. With time, creep of the rock salt is supposed to close the rooms and encapsulate the waste. Various storage options for the waste have been considered.

The disposal room model is developed around a rectangular room 3.96 m high by 10.06 m wide by 91.44 m in length with an initial room free volume of 3644 m^3. The current disposal configuration calls for 6804 drums of uniformly distributed unprocessed waste to be stored in the disposal room in 7-pack units. There are 972 of these units stacked three high along the disposal room floor. Unlike previous calculations which included a crushed salt layer around the waste and in the void space between the drums, the current analyses considered a disposal room with waste only, no backfill. The corresponding volume occupied by the waste and the drums is 1728 m^3.

The transuranic waste form is a combination of metallics, sorbents, cellulose, rubber and plastics, and sludges. Table 1 summarizes the available data for characterizing the waste. The initial waste density, ρ_0, is 559.5 kg/m^3 and the solid waste density, ρ_s, is 1757 kg/m^3. The initial waste density is the sum of the densities of the constituent waste forms. Using the following definition of porosity, ($\phi = 1. - \rho_0 / \rho_s$), the initial waste porosity, ϕ_0, is calculated to be 0.681 resulting in an initial solid volume of 551.2 m^3. Using the initial solid volume allows us to calculate the initial porosity of the undeformed disposal room as 0.849.

Table 1: WIPP CH-TRU Waste Material Parameter Disposal Inventory (Butcher, 1997)

Waste Form	Waste Density (kg/m^3)	Volume Fraction
Metallic	122.	0.218
Sorbents	40.	0.071
Cellulose	170.	0.304
Rubber & Plastics	84.	0.150
Sludges	143.5	0.256
Sum	*559.5*	*0.999*

The gas generation potential and gas production rate corresponding to the reference case are composed of gas from two sources: anoxic corrosion and microbial activity. Butcher

(1997) reports that the estimated gas production potential from anoxic corrosion will be 1050 *moles/drum* with a production rate of 1 *mole/drum/year*. The gas production potential from microbial activity is estimated to be 550 *moles/drum* with a production rate of 1 *mole/drum/year*. This means that microbial activity ceases at 550 years while anoxic corrosion will continue until 1050 years after emplacement. The total amount of gas generated in a disposal room for the reference case was specified to be based on the 6804 unprocessed waste drums per room. The total gas potential for the reference case is shown in Figure 2.

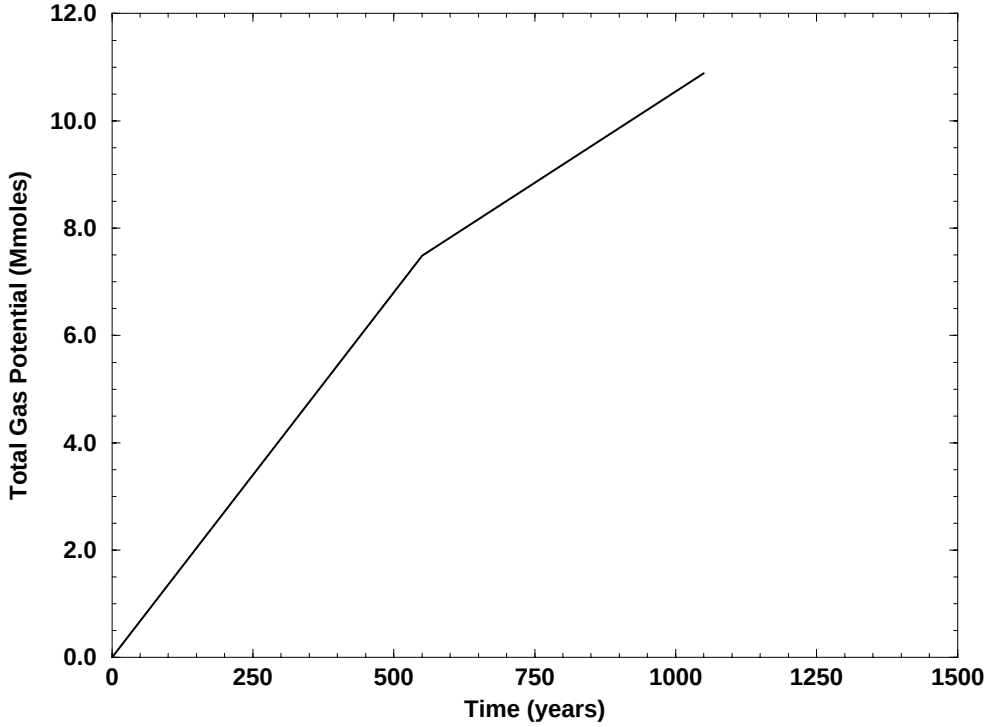


Figure 2. History of the Reference Gas Generation Potential Used for the Disposal Room Analyses, f = 1.0.

The quasistatic, large deformation finite element code SANTOS (Stone, 1997), version 2.0.0 installed on the Sandia Cray J916 computer, was used for the analyses. SANTOS is designed to compute the quasistatic, large deformation, inelastic response of two-dimensional planar or axisymmetric solids. The solution strategy used to obtain the equilibrium states is based on a self-adaptive, dynamic relaxation solution scheme, which is based on explicit central difference pseudo-time integration and artificial mass proportional damping. The explicit nature of the code means that no stiffness matrix is formed or factorized which results in a reduction in the amount of computer storage necessary for execution. The element used in SANTOS is a uniform strain, 4-node, quadrilateral element with an hourglass control scheme to minimize the effects of spurious deformation modes. Finite strain constitutive models for many common engineering materials are available. A robust master-slave contact algorithm for modeling arbitrary sliding contact is implemented.

SANTOS computes the pressure in an enclosed, but deforming volume, with a user supplied pressure-volume relationship and applies the resulting forces to nodes on the enclosure boundary. The gas pressure in the disposal room was computed from the ideal gas law based on the current free volume in the room. Specifically, the gas pressure, p_g, was computed with the following relationship:

$$p_g = f \frac{NRT}{V} \quad , \qquad \text{(EQ 1)}$$

where N, R, and T are the mass of gas in g-moles for the Baseline case, the universal gas constant, and the absolute temperature in degrees Kelvin, respectively. For the current analyses, the absolute temperature is taken to be 300 K. The variable V is the current free volume of the room. During each iteration in the analysis, the current room volume is calculated based on the displaced positions of the nodes on the boundary of the room. The free room volume, *V*, is computed by subtracting the solid volume of the waste, 551.2 m^3, from the current room volume. The gas generation variable, f, is a multiplier used in the analyses to scale the pressure by varying the amount of gas generation. A value of f=1 corresponds to an analysis incorporating full gas generation, while a value of f=0 corresponds to an analysis incorporating no internal pressure increase due to gas generation.

The porosity surface defines the relationship between disposal room porosity, amount of gas present in that porosity, and time. Porosity can be computed directly from the disposal room deformed shape. The concept of the porosity surface comes from the observation that disposal room closure is directly influenced by gas generation and that disposal room closure results for f = 0.8 lie between those for f = 0.6 and f = 1.0. This observation allows a surface to be constructed incorporating the closure results for various values of *f*, which is a convenient way to express the amount of gas generation occurring.

Geomechanical Model

Stratigraphy and Numerical Model

The idealized stratigraphy for the WIPP underground used in the geomechanical model is the stratigraphy as defined by Munson et al. (1989). This stratigraphy is shown in Figure 3 with the disposal room located at the proper horizon. Recent work by Osnes and Labreche, included as an appendix in Butcher (1997), has quantified the differences in room closure obtained by assuming different stratigraphic models which incorporate different numbers of clay seams and anhydrite marker beds. They compared a full stratigraphic model consisting of 12 clay seams and 7 anhydrite layers to analysis results using smaller combinations of clay seams and marker beds. Their work showed that room closure and room porosity results from the full model could be reproduced using the simpler models. In preparing for the current analyses, the author performed a set of calculations (Butcher, 1997) which identified a simple stratigraphic model that captured most of the room closure and room porosity results seen in the more complex stratigraphic models. The stratigraphic model used in the current work is composed of mainly argillaceous salt with a clean salt layer above the disposal room between Clay G and Clay I, anhydrite MB 139, and a thin anhydrite layer located in the clean salt layer identified as anhydrite A. Based on the prior study by the author (Butcher, 1997), no clay seams were included in the model. The final stratigraphic model used for the analyses is shown in Figure 4.

A two-dimensional plane strain disposal room model, as shown in Figure 5, was used for the SANTOS analyses. The discretized model represents the room as one of an infinite number of rooms located at the repository horizon. Making use of symmetry, only half of the room needed to be modeled. The left and right boundaries are planes of symmetry. The upper and lower boundaries are located approximately 50 m from the room. A lithostatic stress ($\sigma_x = \sigma_y = \sigma_z$) that varies with depth is used as the initial stress on the configuration and gravity forces are included. The model contains 1,680 quadrilateral uniform-strain elements and 1,805 nodal points. A zero-displacement boundary condition in the horizontal direction (Ux = 0.0) was applied on both the left and right boundaries of the model to represent the symmetry condition of a half-symmetry disposal room in an infinite array of rooms. A prescribed normal traction of 13.57 MPa was applied on the upper boundary and a vertical zero-displacement boundary condition (Uy = 0.0) was applied on the lower boundary to react the overburden load. An adaptive internal pressure, p_g, was applied around the boundary of the disposal room.

The basic half-symmetry disposal room dimensions are 3.96 m high by 5.03 m wide with a significant portion of this area containing the stored CH-TRU waste. The waste is stored in 7-packs stacked three high along the drift with a height of 2.676 m. This storage configuration contains a large amount of void volume associated with each 7-pack. To obtain the waste volume dimensions used in the calculations, the assumption is made that each waste drum will laterally deform independent of one another. This void space between drums must be eliminated in order to have an accurate continuum representation of the

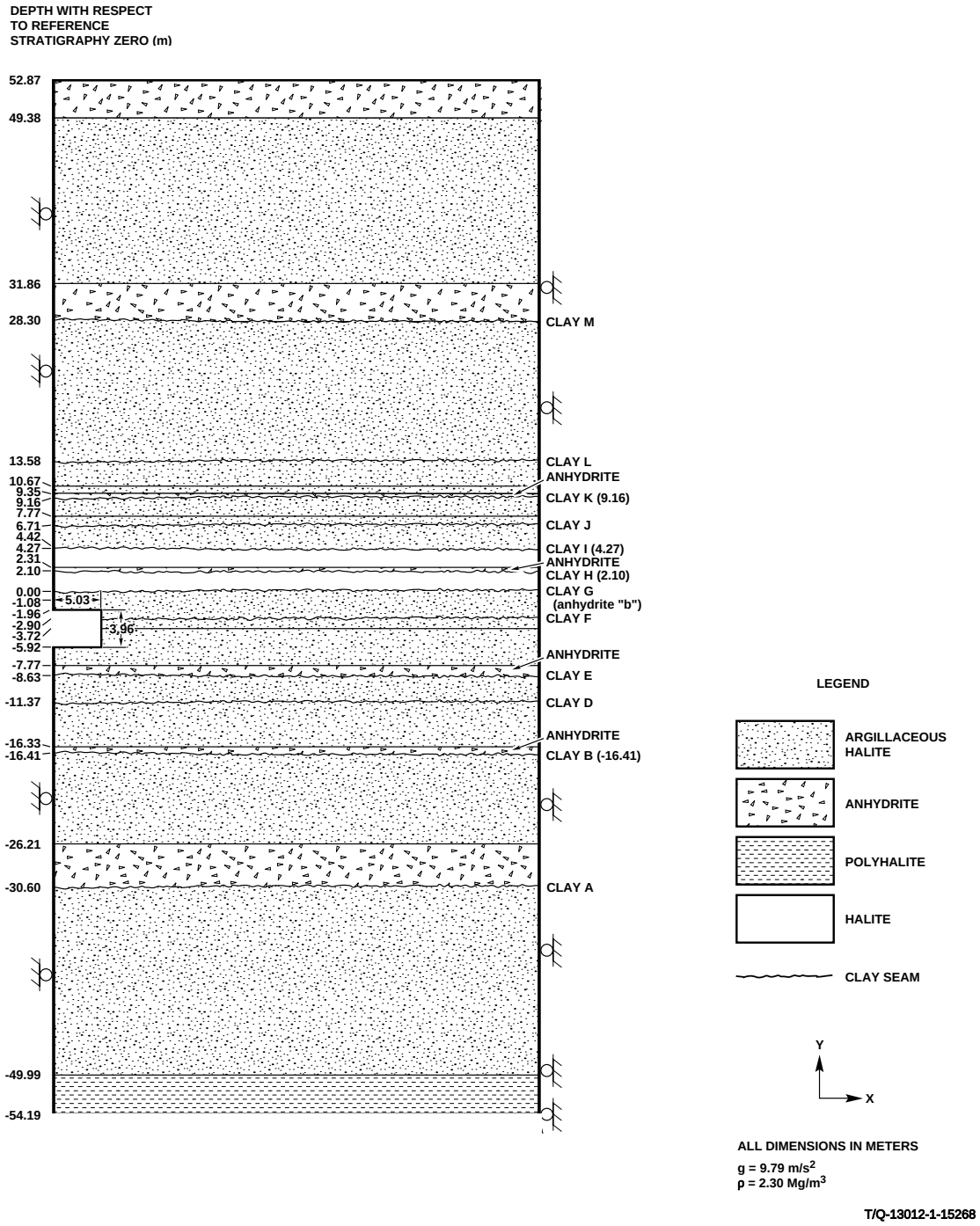


Figure 3. Idealized Stratigraphy Near the Disposal Room Horizon Defined by Munson et al. (1989).

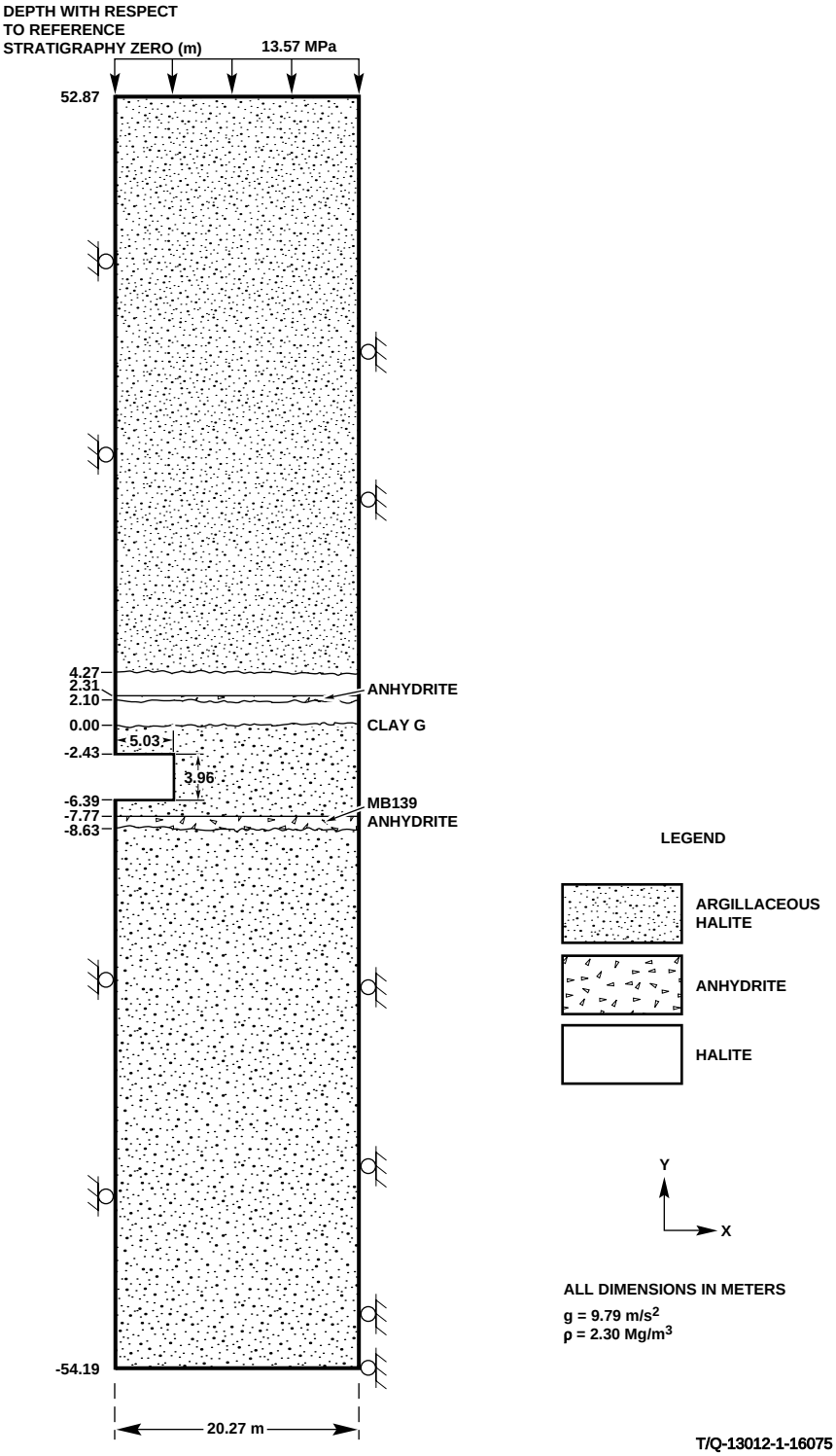


Figure 4. Simplified Statigraphic Model Used For the Current Disposal Room Analyses (Butcher, 1997).

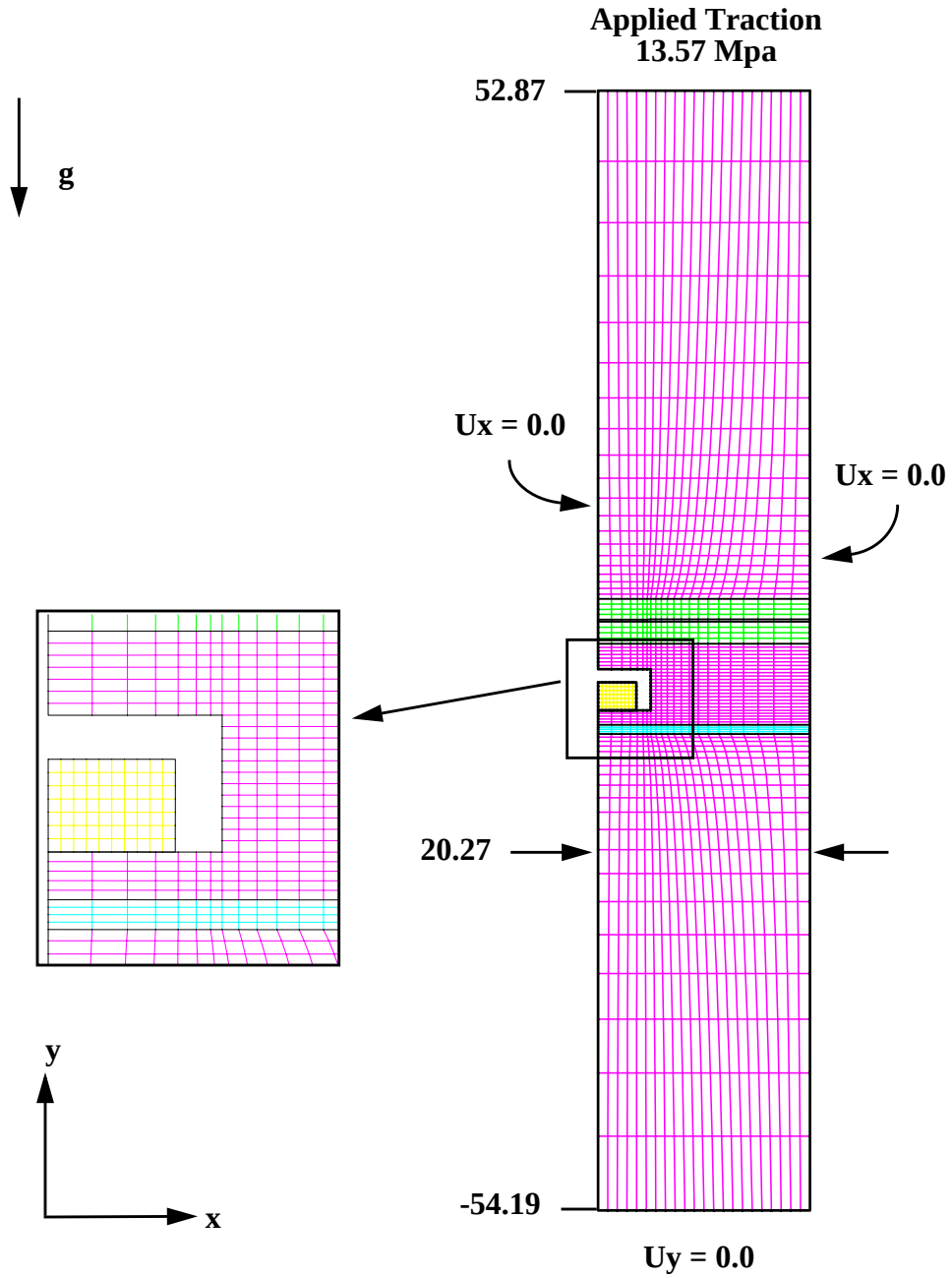


Figure 5. Mesh Discretization and Boundary Conditions Used for the Disposal Room Analyses.

waste response. To eliminate the void space between drums, the assumption is made that the lateral deformation of a configuration of drums caused by inward movement of the walls of the disposal room is sufficient to eliminate space between the drums early in the closure process at low stress levels. In other words, the lateral deformation of the disposal room rib compresses the 7-packs causing the void space between the drums to be removed with little or no resistance by the waste drums themselves. This assumption allows calculation of an effective lateral dimension for the waste after lateral collapse of the space between the drums is complete. The lateral dimension of the waste drums within the disposal room is determined from the total initial waste volume of 1728 m^3. Equation 2 was used to determine the compressed dimensions of the waste used for the continuum representation. In this equation, W_0 is the nominal uncompressed width of the stored waste in the disposal room (8.6 m), L_0 is the nominal length of the disposal room available for storing waste (89.1 m), and H_0 is the height of the three stacked waste containers (2.676 m). The quantity D in Equation 2 is the amount of space that must be eliminated between the drums. Note in Equation 2 that we have chosen to modify the length of the disposal room by the same amount, D. Solving for D, we find that the modified width of the waste is 7.35 m and the modified length is 87.85 m.

$$(W_0 - 2D)(L_0 - 2D)H_0 = 1728 \qquad \text{(EQ 2)}$$

Contact surfaces were defined between the waste and room boundaries to model the contact and sliding that occurs as the room deforms and entombs the waste. Specifically, contact surfaces were defined between the waste and floor of the room, the waste and room rib, and the waste and ceiling. All of the contacts surfaces were allowed to separate if the forces between the surfaces reached a tensile value. This feature allows the room to reopen due to gas generation within the disposal room.

Halite Constitutive Model

A combined transient-secondary creep constitutive model for rock salt attributed to Munson and Dawson (1982) and described by Munson et al. (1989) was used for the clean and argillaceous salt. The model can be decomposed into an elastic volumetric part defined by,

$$\varepsilon_{kk} = \frac{\sigma_{kk}}{3K} , \qquad \text{(EQ 3)}$$

(where the ε_{ij} and the σ_{ij} are the total strain and stress components, respectively, and K is the elastic bulk modulus) and a deviatoric part defined by,

$$\dot{s}_{ij} = 2G\left(\dot{e}_{ij} - F\dot{\varepsilon}_s\left[\frac{\cos 2\theta}{\cos 3\theta\sqrt{J_2}}s_{ij} - \frac{\sqrt{3}\sin\theta}{\cos 3\theta J_2}\left\{s_{ip}s_{pj} - \frac{2J_2}{3}\delta_{ij}\right\}\right]\right) , \qquad \text{(EQ 4)}$$

where the second term of the above equation represents the creep contribution. In the above equation, s_{ij} is the deviatoric stress defined as $s_{ij} = \sigma_{ij} - \frac{\sigma_{kk}}{3}$, G is the elastic shear modulus, and e_{ij} is the deviatoric strain defined by $e_{ij} = \varepsilon_{ij} - \frac{\varepsilon_{kk}}{3}$.

In the creep term of Equation 4, F is a multiplier on the steady-state creep rate to simulate the transient creep response according to the following,

$$F = \begin{cases} e^{\Delta[1-\zeta/\varepsilon_t^*]^2}, & \zeta < \varepsilon_t^* \\ 1, & \zeta = \varepsilon_t^* \\ e^{-\delta[1-\zeta/\varepsilon_t^*]^2}, & \zeta > \varepsilon_t^* \end{cases}, \qquad \text{(EQ 5)}$$

where Δ and δ are work-hardening and recovery parameters, respectively, and ε_t^* is the so-called transient strain limit. Finally, ζ is an internal state variable whose rate of change is determined by the following evolutionary equation,

$$\dot{\zeta} = (F-1)\dot{\varepsilon}_s . \qquad \text{(EQ 6)}$$

In Equation 5, the work-hardening parameter Δ is defined as $\Delta = \alpha + \beta\log(\bar{\sigma}/G)$ where α and β are constants. The variable $\bar{\sigma}$ is the equivalent Tresca stress given by $\bar{\sigma} = 2\sqrt{J_2}\cos\theta$ where $\theta = \frac{1}{3}\text{asin}\left[\frac{-3\sqrt{3}J_3}{2(J_2)^{3/2}}\right]$ is the Lode angle and is limited to the range $-\frac{\pi}{6} \le \theta \le \frac{\pi}{6}$. The variables J_2 and J_3 are the second and third invariants of the stress deviator given by $J_2 = \frac{1}{2}s_{pq}s_{qp}$ and $J_3 = \frac{1}{3}s_{pq}s_{qr}s_{rp}$, respectively. The recovery parameter δ is held constant. The transient strain limit is given by $\varepsilon_t^* = K_o e^{cT}(\bar{\sigma}/G)^M$ where K_o, c, and M are constants.

The steady-state, or secondary creep, strain rate, $\dot{\varepsilon}_s$, is given by

$$\dot{\varepsilon}_s = A_1 e^{-Q_1/RT}\left(\frac{\bar{\sigma}}{G}\right)^{n_1} + A_2 e^{-Q_2/RT}\left(\frac{\bar{\sigma}}{G}\right)^{n_2} + |H|[B_1 e^{-Q_1/RT} + B_2 e^{-Q_2/RT}]\sinh\left[\frac{q(\bar{\sigma}-\sigma_o)}{G}\right]; \qquad \text{(EQ 7)}$$

where the A_is and B_is are constants, the Q_is are activation energies, T is the absolute temperature, R is the universal gas constant, the n_is are the stress exponents, q is the so-called stress constant, σ_o is the stress limit of the dislocation slip mechanism, and $|H|$ is the Heaviside step function with the argument $(\bar{\sigma} - \sigma_o)$. The material constants corresponding to the clean and argillaceous salt, used in the analyses, are given in Table 2 and Table 3.

Table 2: Salt Elastic Properties (Butcher, 1997)

G MPa	E MPa	ν
12,400	31,000	0.25

Table 3: Salt Creep Properties (Butcher, 1997)

Parameters (units)	Clean Salt	Argillaceous Salt
A_1 (/sec)	8.386E22	1.407E23
Q_1 (cal/mole)	25,000	25,000
n_1	5.5	5.5
B_1 (/sec)	6.086E6	8.998E6
A_2 (/sec)	9.672E12	1.314E13
Q_2 (cal/mole)	10,000	10,000
n_2	5.0	5.0
B_2 (/sec)	3.034E-2	4.289E-2
σ_o (MPa)	20.57	20.57
q	5,335	5,335
m	3.0	3.0
K_o	6.275E5	2.470E6
c (/T)	9.198E-3	9.198E-3
α_w	-17.37	-14.96
β_w	-7.738	-7.738
δ	0.58	0.58

Waste Constitutive Model

The stress-strain behavior of the waste was represented by a volumetric plasticity model (Stone, 1997) with a piecewise linear function defining the relationship between the mean stress and the volumetric strain. Compaction experiments on simulated waste were used to develop this relationship. The deviatoric response of the waste material has not been characterized. It is anticipated that when a drum filled with loosely compacted waste is compressed axially, the drum will not undergo significant lateral expansion until most of the void space inside the drum has been eliminated.

For the volumetric plasticity model, the yield surface in principal stress space is a surface of revolution with its axis centered about the hydrostat and the open end pointing into the compression direction. The open end is capped with a plane which is at right angles to the hydrostat. The deviatoric part is elastic-perfectly plastic so the surface of revolution is stationary in stress space. The volumetric part has variable strain hardening so the end plane moves outward during volumetric yielding. The volumetric hardening is defined by a set of pressure-volumetric strain relations. A flow rule is used such that deviatoric strains produce no volume change (associated flow). The model is best broken into volumetric and deviatoric parts with the deviatoric part resembling conventional plasticity. The volumetric yield function is a product of two functions, ϕ_s and ϕ_p, describing the surface of revolution and the plane normal to the pressure axis, respectively. These are given by

$$\phi_s = \frac{1}{2}s_{ij}s_{ij} - a_0 + a_1 p + a_2 p^2 \qquad \text{(EQ 8)}$$

$$\phi_p = p - g(\varepsilon_v) \qquad \text{(EQ 9)}$$

where a_0, a_1, a_2 are constants defining the deviatoric yield surface, p is the pressure, and ε_v is the volume strain. The form of g is defined in this problem by a set of piecewise linear segments relating pressure-volume strain. Table 4 lists the pressure-volumetric strain data used for the waste drum model and the data is plotted in Figure 6. Note that the final point listed in the table is a linear extrapolation beyond the curve data given in Butcher (1997). The final pressure of 12 Mpa corresponds to an axial stress on a waste drum of 36 Mpa. The elastic material parameters and constants defining the yield surface are given in Table 5.

Anhydrite Constitutive Model

The anhydrite layer beneath the disposal room is expected to experience inelastic material behavior. The MB 139 anhydrite layer is considered to be isotropic and elastic until yield occurs. Once the yield stress is reached, plastic strain begins to accumulate. Yield is assumed to be governed by the Drucker-Prager criterion

$$\sqrt{J_2} = C - aJ_1 \qquad \text{(EQ 10)}$$

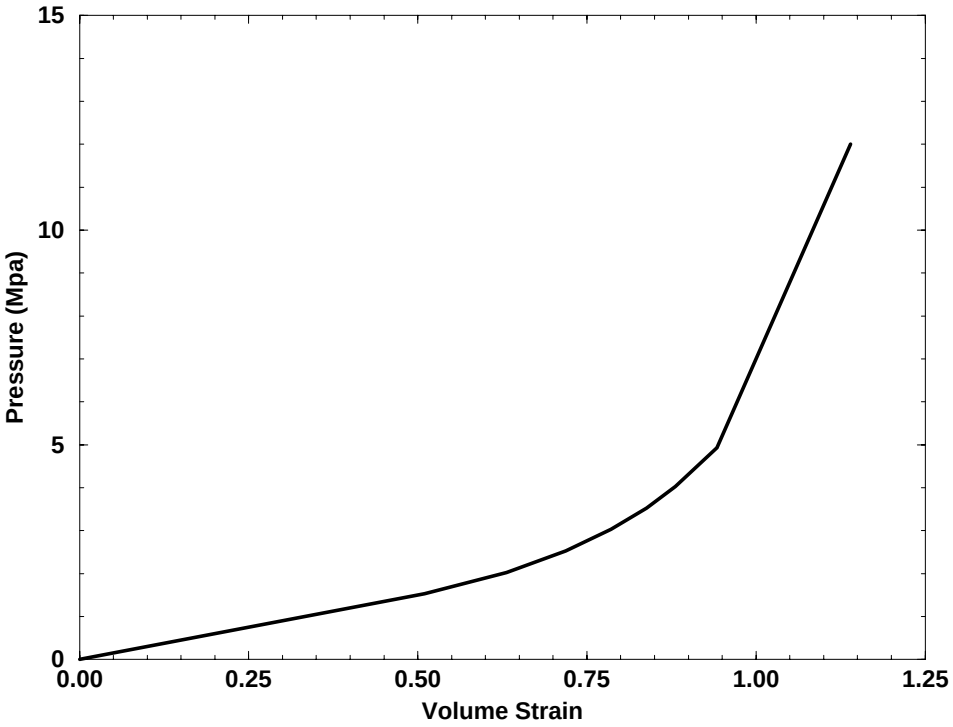


Figure 6. Curve of the Pressure-Bulk Strain Input to the Volumetric Plasticity Model Used to Model the Waste Drums

Table 4: Pressure-Volumetric Strain Data Used in the Volumetric-Plasticity Model for the Waste Drums (Butcher, 1997)

Pressure (MPa)	$\ln(\rho/\rho_0)$
1.53	0.510
2.03	0.631
2.53	0.719
3.03	0.786
3.53	0.838
4.03	0.881
4.93	0.942
12.0	1.14

Table 5: Material Constants Used With the Volumetric Plasticity Model for the Waste (Butcher, 1997)

Parameter	Value
G	333. Mpa
K	222 Mpa
a_0	1.0 Mpa
a_1	3.0
a_2	0.

where J_2 is the second deviatoric stress invariant and J_1 is the first stress invariant (σ_{kk}). A nonassociative flow rule is used to determine the plastic strain components. The elastic properties and Drucker-Prager constants, C and a, for the anhydrite are given in Table 6.

Table 6: Elastic and Drucker-Prager Constants for Anhydrite (Butcher, 1997)

Material	Young's Modulus (Gpa)	Poisson's Ratio	C (Mpa)	a
Anhydrite	75.1	0.35	1.35	0.45

Results of the Analyses

Analyses using SANTOS, version 2.0.0 installed on the Sandia Cray J916, were carried out to a simulation time of 10,000 years. Thirteen cases of gas generation were investigated, these were for f=0.0, 0.025, 0.05, 0.1, 0.2, 0.4, 0.5, 0.6, 0.8, 1.0, 1.2, 1.6, and 2.0. The input file for one of the SANTOS analyses is included in Appendix A. The other input files are identical except for the title line. The gas generation parameter, *f*, is set in the user-supplied subroutine FPRES. A sample FPRES subroutine for f = 2.0 is given in Appendix B.

The results of interest from the analyses are the pressure buildup in the disposal room and the corresponding room porosity. Figure 7 shows the disposal room pressure histories for the various values of gas generation parameter, f. Obviously for f=0, the amount of gas generation is zero resulting in a zero pressure in the room for all times. As would be expected in all other cases, the room pressure rises during the gas generation period of 1,050 years. Thereafter in time, there appears to be a transition in the character of the response at about f=0.5. For f values greater than 0.5, the room pressure begins to drop after gas generation stops, and for values less than 0.5, the room pressure remains constant throughout the 10,000 year simulation. For example with f=1.0 (full gas generation) the room pressure increases monotonically during the period of gas generation and reaches a value slightly larger than 21 MPa at 1,050 years. When the gas generation ceases at this time, the room pressure begins to drop, reaching a value of approximately 18 MPa at 10,000 years. For the highest values of f (1.6 and 2.0), there is very little difference in the maximum pressure reached, approximately 23 Mpa at 550 years. The pressure drops dramatically to 18 Mpa at 10,000 years and still appears to be decreasing as the internal gas pressure and overburden try to reach equilibrium. On the other end of the range for f, an interesting case is f=0.025 (i.e., 2.5 percent of full gas generation). The figure clearly shows that for even this tiny amount of gas generation, the pressure in the room rises significantly (3 MPa at the end of 10,000 years) to approximately 20 % of the value of the lithostatic stress at the repository horizon.

Figure 8 shows the disposal room porosity histories for the thirteen cases of gas generation considered. As would be expected, the room porosity drops monotonically from its initial value of approximately 85 percent for the first 100 to 500 years, depending on the value of f. Thereafter, once again, there appears to be a transition in response at about f=0.5. For values of f below that value, the porosity continues to decrease with time but at a slower rate, as equilibrium is reached between the internal gas pressure and the salt overburden. For values of f greater than 0.5, the porosity starts to increase after reaching a minimum value. In fact, for the gas generation case of f=2.0, the room actually inflates to a porosity of about 85 percent at the end of the simulation, which is nearly equal to the original porosity. The porosity reached at this same time for the case without any gas generation, f=0, is approximately 23.5 percent.

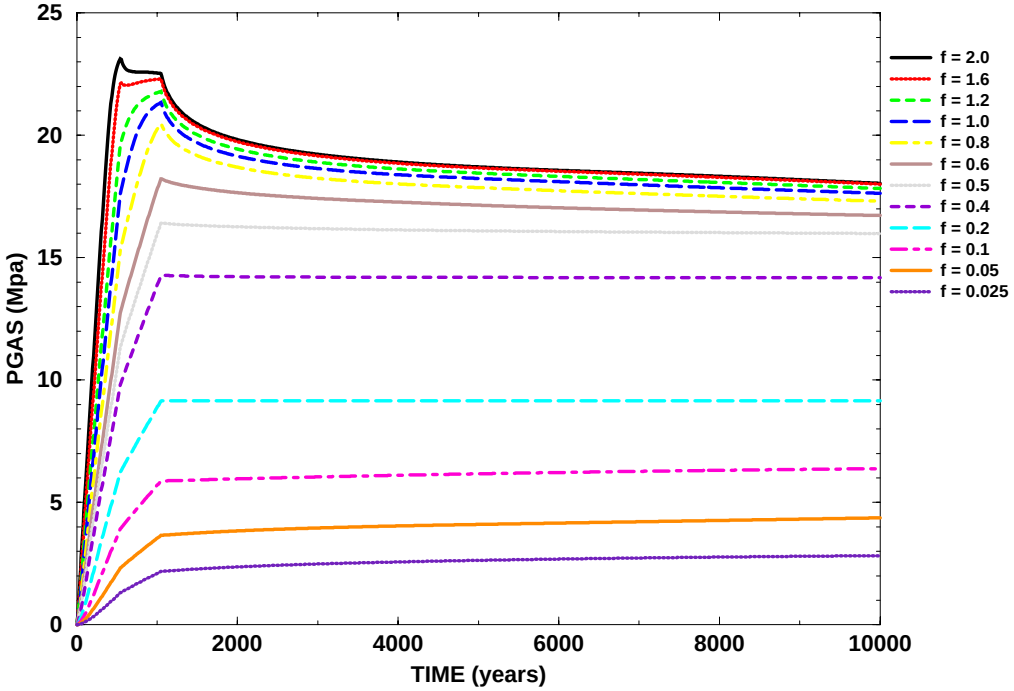


Figure 7. Pressure Histories for Various Values of the Gas Generation Parameter, f, for a Disposal Room Containing Waste Only. The Gas Generation Parameter Values Range From Bottom to Top: f = 0.025, 0.05, 0.10, 0.20, 0.40, 0.50, 0.60, 0.80, 1.0, 1.2, 1.6, and 2.0.

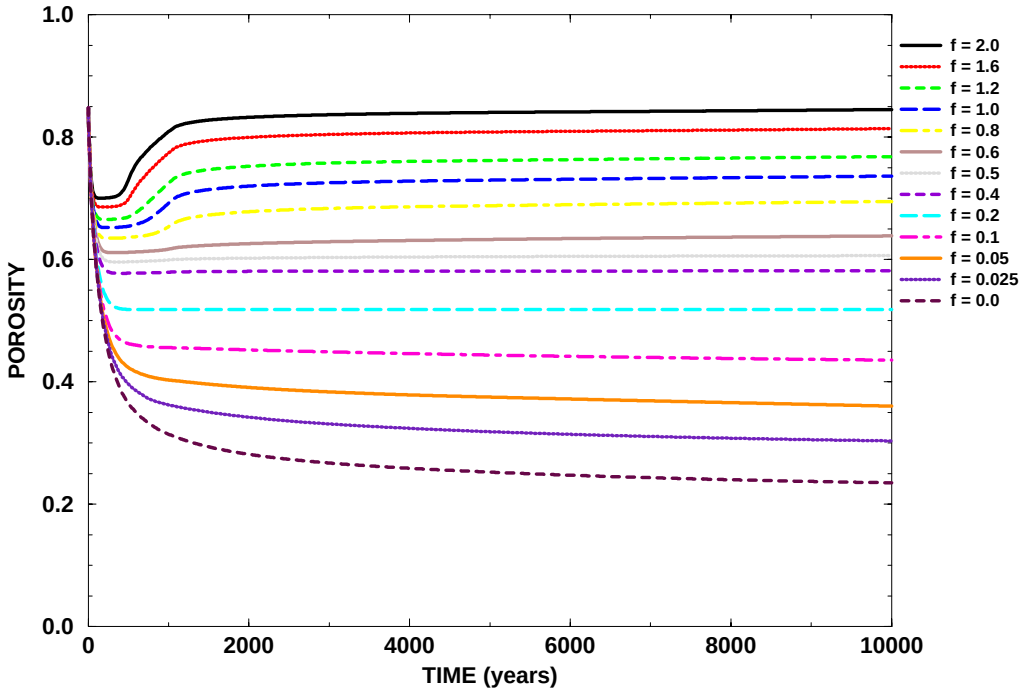


Figure 8. Porosity Histories for Various Values of the Gas Generation Parameter, f, for a Disposal Room Containing Waste Only. The Gas Generation Parameter Values Range From Bottom to Top: f = 0.0, 0.025, 0.05, 0.10, 0.20, 0.40, 0.50, 0.60, 0.80, 1.0, 1.2, 1.6, and 2.0.

Figure 9 and Figure 10 show a close-up view of the deformed mesh around the disposal room at 300 and 10,000 years, respectively, for $f = 0.0$. The deformed shape clearly shows that the maximum compaction of the waste is due to vertical closure of the room. At 300 years the vertical closure has reached 77 percent of its maximum value. Horizontal contact of the rib with the waste occurs at approximately 150 years. At 10,000 years, the waste has been compacted somewhat by horizontal closure of the rib but not significantly compared to the vertical compaction. Both figures show that the large deformations of the roof and floor result in contact with the rib at the corners of the room. The contact in the corners of the disposal room is an important feature of the analyses and the arbitrary contact surface capability in SANTOS allows it to be captured. The roof and floor are either in contact with the waste or in contact with each other which means that no significant void spaces are developed. This deformation mode results in a minimum free volume in the room.

The closure of the disposal room at 300 and 10,000 years for $f = 0.5$ is shown in Figure 11 and Figure 12, respectively. As seen in the figures, the compaction of the waste is entirely due to vertical room closure since the deforming rib does not come into contact with the waste. No contact between the waste and rib occurs at any time during the $f = 0.5$ analysis. The gas generation is such that the room porosity is the same at 300 years as at 10000 years. The gas pressure essentially balances the overburden load so that the vertical closure of the disposal room becomes constant.

.

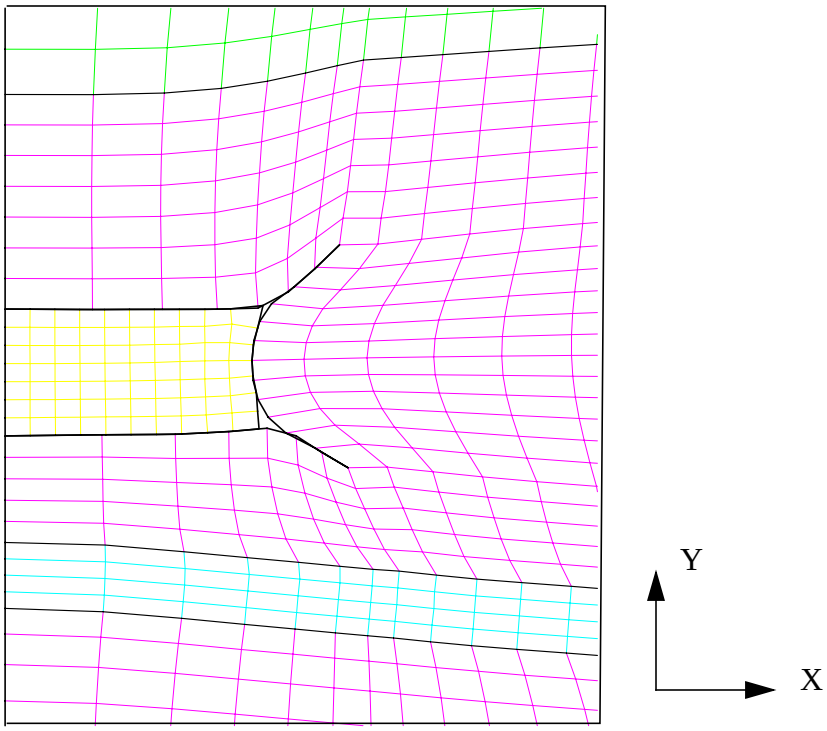


Figure 9. Close-up View of the Deformed Disposal Room With Waste at 300 Years for $f = 0.0$.

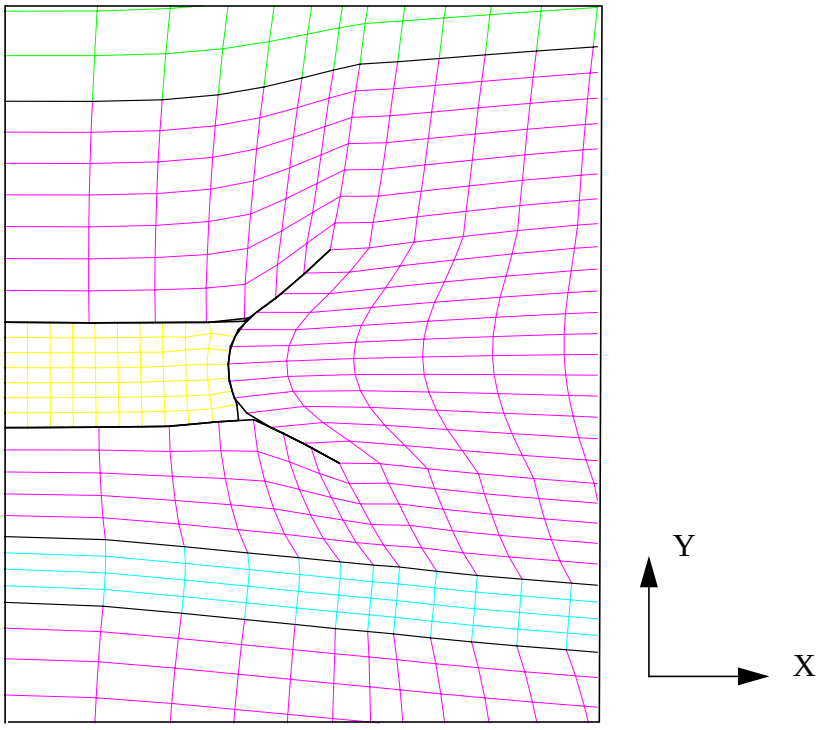


Figure 10. Close-up View of the Deformed Disposal Room With Waste at 10,000 Years for $f = 0.0$.

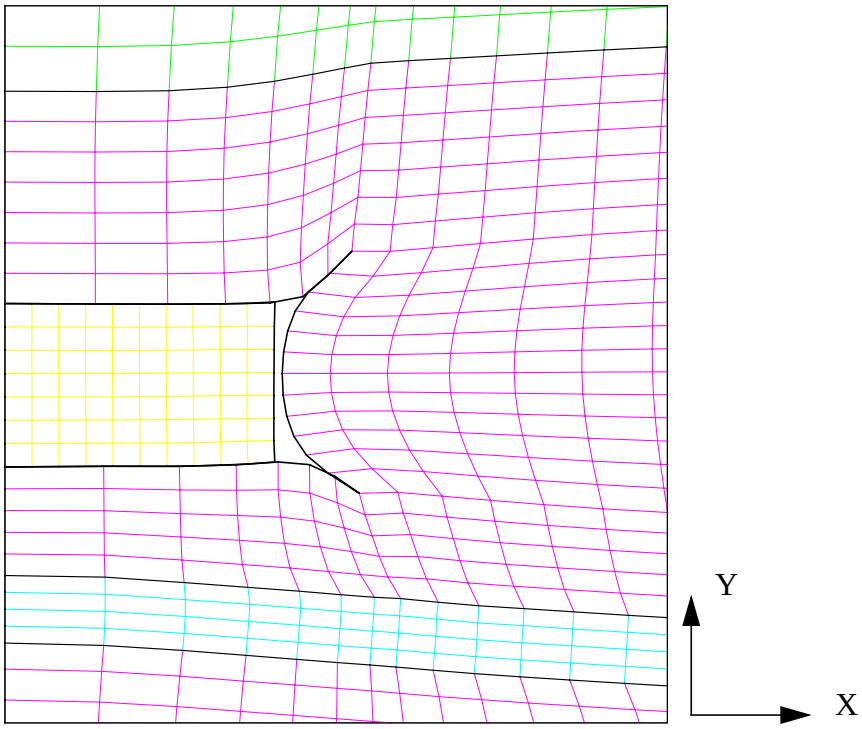


Figure 11. Close-up View of the Deformed Disposal Room With Waste at 300 Years for f = 0.5.

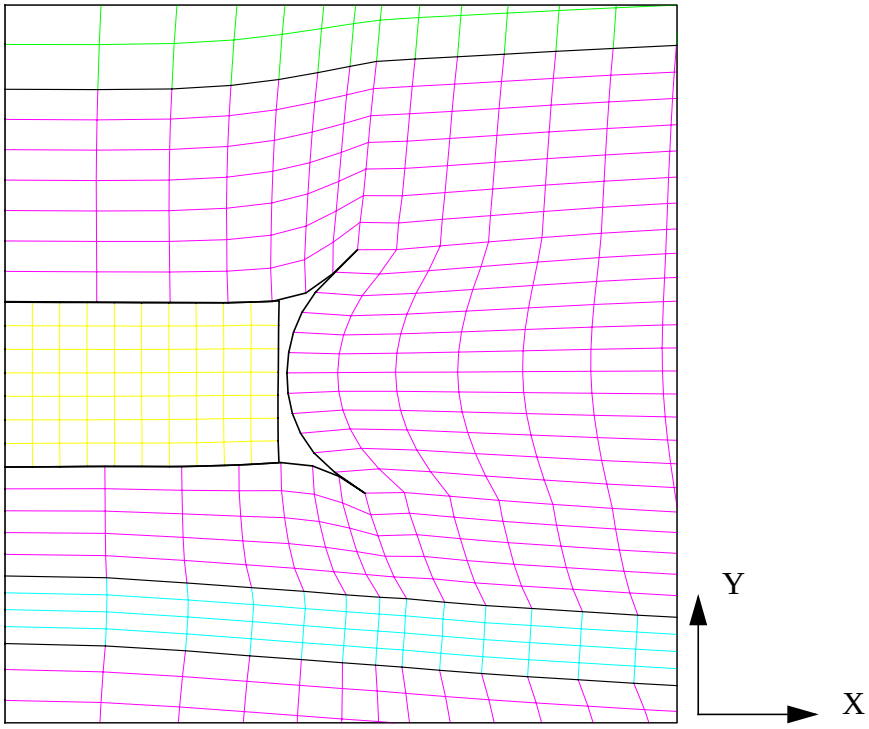


Figure 12. Close-up View of the Deformed Disposal Room With Waste at 10,000 Years for f = 0.5.

Summary of Results

Calculations of the mechanical creep closure response of a disposal room with waste but without crushed salt backfill have been performed to allow three-dimensional porosity surfaces to be constructed for WIPP performance assessment activities. Data supplied to the performance assessment group consisted of room pressure and porosity histories for various gas generation rates for a period of 10,000 years following excavation and waste emplacement. Closure results from the calculations show rapid closure of the disposal room occurring during the first 100 to 500 years following excavation. Depending upon the amount of gas generation, the room will either continue to experience a decrease in porosity over time due to continued creep closure of the room or an increasing porosity due to the action of the internally generated pressure acting on the room boundaries.

References

Bertram-Howery, S.G., M.G. Marietta, R.P. Rechard, D.R. Anderson, and P.N. Swift. 1990. *Preliminary Comparison with 40 CFR Part 191, Subpart B for the Waste Isolation Pilot Plant, December 1990.* SAND90-2347. Albuquerque, NM: Sandia National Laboratories.

Butcher, B.M., and F.T. Mendenhall. 1993. *Summary of the Models Used for the Mechanical Response of Disposal Rooms in the Waste Isolation Pilot Plant with Regard to Compliance with 40 CFR 191, Subpart B.* SAND92-0427. Albuquerque, NM: Sandia National Laboratories.

Butcher, B.M. 1997. *A Summary of the Sources of Input Parameter Values for the WIPP Final Porosity Surface Calculations*. SAND97-0796, Albuquerque, NM: Sandia National Laboratories.

EPA (Environmental Protection Agency). 1985. "40 CFR 191: Environmental Standards for the Management and Disposal of Spent Nuclear Fuel, High-Level and Transuranic Radioactive Wastes; Final Rule," *Federal Register.* Vol. 50, no. 182, 38066 - 38089.

Munson, D.E., and P.R. Dawson. 1982. *A Transient Creep Model for Salt During Stress Loading and Unloading*. SAND82-0962. Albuquerque, NM: Sandia National Laboratories.

Munson, D.E., A.F. Fossum, and P.E. Senseny. 1989. *Advances in Resolution of Discrepancies Between Predicted and Measured In Situ WIPP Room Closures*. SAND88-2948. Albuquerque, NM: Sandia National Laboratories.

Stone, C.M. 1997. SANTOS – *A Two-Dimensional Finite Element Program for the Quasistatic, Large Deformation, Inelastic Response of Solids*. SAND90-0543. Albuquerque, NM: Sandia National Laboratories.

Appendix A:

Sample SANTOS Input File for a Disposal Room Analysis

```
TITLE
DISPOSAL ROOM CALCULATION - FINAL - F = 2.0 - WASTE W/O BACKFILL
PLANE STRAIN
INITIAL STRESS = USER
GRAVITY = 1 = 0. = -9.79 = 0.
PLOT ELEMENT, STRESS, STRAIN, VONMISES, PRESSURE
PLOT NODAL, DISPLACEMENT, RESIDUAL
PLOT STATE, EQCS, EV
RESIDUAL TOLERANCE = 0.5
MAXIMUM ITERATIONS = 1000
MAXIMUM TOLERANCE = 100.
INTERMEDIATE PRINT = 100
ELASTIC SOLUTION
PREDICTOR SCALE FACTOR = 3
AUTO STEP .015 2.592E6 NOREDUCE 1.E-5
TIME STEP SCALE = 0.5
HOURGLASS STIFFENING = .005
STEP CONTROL
   500  3.1536e7
  2000  3.1536e9
 36000  3.1536e11
END
OUTPUT TIME
   1   3.1536e7
   1   3.1536e9
 200   3.1536e11
END
PLOT TIME
  10   3.1536e7
 100   3.1536e9
 120   3.1536e11
END
 MATERIAL, 1, M-D CREEP MODEL, 2300. $ ARGILLACEOUS HALITE
TWO MU = 24.8E9
BULK MODULUS = 20.66E9
A1 = 1.407E23
Q1/R = 41.94
N1 = 5.5
B1 = 8.998E6
A2 = 1.314E13
Q2/R = 16.776
N2 = 5.0
B2 = 4.289E-2
SIG0 = 20.57E6
QLC = 5335.
M = 3.0
K0 = 2.47E6
C = 2.759
ALPHA = -14.96
BETA = -7.738
DELTLC = .58
RN3 = 2.
AMULT = .95
END
```

```
MATERIAL, 2, SOIL N FOAMS, 2300.   $ ANHYDRITE
TWO MU = 5.563E10
BULK MODULUS = 8.3444E10
A0 = 2.338e6
A1 = 2.338
A2 = 0.
PRESSURE CUTOFF = 0.0
FUNCTION ID = 0
END
 MATERIAL, 3, M-D CREEP MODEL, 2300. $ PURE HALITE
TWO MU = 24.8E9
BULK MODULUS = 20.66E9
A1 = 8.386E22
Q1/R = 41.94
N1 = 5.5
B1 = 6.086E6
A2 = 9.672E12
Q2/R = 16.776
N2 = 5.0
B2 = 3.034E-2
SIG0 = 20.57E6
QLC = 5335.
M = 3.0
K0 = 6.275E5
C = 2.759
ALPHA = -17.37
BETA = -7.738
DELTLC = .58
RN3 = 2.
AMULT = .95
END
MATERIAL, 4, SOIL N FOAMS, 752.
TWO MU = 3.333E8
BULK MODULUS = 2.223E8
A0 = 1.0e6
A1 = 3.
A2 = 0.
PRESSURE CUTOFF = 0.
FUNCTION ID = 2
END
NO DISPLACEMENT X = 1
NO DISPLACEMENT Y = 2
PRESSURE, 10, 1, 13.57E6
CONTACT SURFACE, 100, 400, 0., 1.E-3, 1.E40
CONTACT SURFACE, 200, 500, 0., 1.E-3, 1.E4
CONTACT SURFACE, 300, 600, 0., 1.E-3, 1.E4
CONTACT SURFACE, 300, 200, 0., 1.E-3, 1.E4
CONTACT SURFACE, 100, 200, 0., 1.E-3, 1.E4
ADAPTIVE PRESSURE, 700, 1.e-6, -6.4
FUNCTION,1  $ FUNCTION TO DEFINE PRESCRIBED PRESSURE
0., 1.
3.1536e11, 1.
END
FUNCTION,2
```

```
 0.0000, 0.0000
 0.5101, 1.5300E6
 0.6314, 2.0307E6
 0.7189, 2.5321E6
 0.7855, 3.0312E6
 0.8382, 3.5301E6
 0.8808, 4.0258E6
 0.9422, 4.9333E6
 1.1400, 12.000E6
END
FUNCTION = 3
 0.        0.5
 3.1536E11 1.
END
EXIT
```

Appendix B:

Sample User Subroutines for the Adaptive Pressure Boundary Condition and the Initial Stress State

```
      SUBROUTINE FPRES( VOLUME,TIME,PGAS )
C ....
C .... THE PRESSURE IS COMPUTED ON THE BASIS OF THE IDEAL GAS LAW,
C .... PV = NRT. THE TOTAL NUMBER OF MOLES OF GAS, N (EN), PRESENT
C .... AT ANY TIME IS DETERMINED ON THE BASIS OF A CONSTANT RATE OF GAS
C .... GENERATION. R IS THE UNIVERSAL GAS CONSTANT AND THETA IS THE ROOM
C .... TEMPERATURE, 300 K. V IS THE CURRENT VOLUME OF THE ROOM. THE VOLUME
C .... MUST BE CORRECTED BY MULTIPLYING BY 2 OR 4 TO ACCOUNT FOR THE USE OF
C .... HALF OR QUARTER-SYMMETRY MODELS. THE VOLUME MUST ALSO BE MULTIPLIED
C .... BY A FACTOR TO ACCOUNT FOR 3D LENGTH.
C ....
C
      R = 8.314
      THETA = 300.
C
      IF( TIME .LT. 1.7325E10 )THEN
         PVALUE = 0.0
         RATE = 4.32E-4
         TSTAR = 0.0
      ELSE IF( TIME .LT. 3.3075E10 )THEN
         PVALUE = 7.48E6
         RATE = 2.16E-4
         TSTAR = 1.7325E10
      ELSE
         PVALUE = 1.0886e7
         RATE = 0.0
         TSTAR = 0.0
      END IF
C
C .... CORRECT VOLUME AT THIS TIME TO GET VOLUME OF VOIDS
C
      EN = PVALUE + RATE * ( TIME - TSTAR )
      SCALE = 2.
      SYMFAC = 2.
      XLENG = 91.44
C
C     .... THIS MODIFICATION REMOVES THE BACKFILL FROM VSOLID
C
C     VSOLID FOR WASTE AND DRUMS ONLY 551.2
      VSOLID = 551.2
      VOLUME = SYMFAC * VOLUME * XLENG - VSOLID
      IF( VOLUME .LE. 0.0 )VOLUME = 1.
C
      PGAS = SCALE * EN * R * THETA / VOLUME
C
      RETURN
      END
```

```
      SUBROUTINE INITST( SIG,COORD,LINK,DATMAT,KONMAT,SCREL )
C
C
*****************************************************************
C
C   DESCRIPTION:
C     THIS ROUTINE PROVIDES AN INITIAL STRESS STATE TO SANTOS
C
C   FORMAL PARAMETERS:
C    SIG     REAL       ELEMENT STRESS ARRAY WHICH MUST BE RETURNED
C                           WITH THE REQUIRED STRESS VALUES
C     COORD    REAL        GLOBAL NODAL COORDINATE ARRAY
C     LINK     INTEGER     CONNECTIVITY ARRAY
C     DATMAT   REAL        MATERIAL PROPERTIES ARRAY
C     KONMAT   INTEGER     MATERIAL PROPERTIES INTEGER ARRAY
C
C   CALLED BY: INIT
C
*****************************************************************
C
      INCLUDE 'params.blk'
      INCLUDE 'psize.blk'
      INCLUDE 'contrl.blk'
      INCLUDE 'bsize.blk'
      INCLUDE 'timer.blk'
C
      DIMENSION LINK(NELNS,NUMEL),KONMAT(10,NEMBLK),
     *        COORD(NNOD,NSPC),SIG(NSYMM,NUMEL),DATMAT(MCONS,*),
     *        SCREL(NEBLK,*)
C
      DO 1000 I = 1,NEMBLK
         MATID = KONMAT(1,I)
         MKIND = KONMAT(2,I)
         ISTRT = KONMAT(3,I)
         IEND = KONMAT(4,I)
            DO 500 J = ISTRT,IEND
               II = LINK( 1,J )
               JJ = LINK( 2,J )
               KK = LINK( 3,J )
               LL = LINK( 4,J )
               ZAVG = 0.25 * ( COORD(II,2) + COORD(JJ,2) +
     *                COORD(KK,2) + COORD(LL,2) )
              STRESS = - 2300. * 9.79 * ( 655. - ZAVG )
               IF( MATID .EQ. 4 )THEN
                  STRESS = 0.
               END IF
               SIG(1,J) = STRESS
               SIG(2,J) = STRESS
               SIG(3,J) = STRESS
               SIG(4,J) = 0.0
  500       CONTINUE
 1000 CONTINUE
      RETURN
      END
```

WIPP
UC721 - DISTRIBUTION LIST
SAND97-0795

Federal Agencies

US Department of Energy (4)
Office of Civilian Radioactive Waste Mgmt.
Attn: Deputy Director, RW-2
Acting Director, RW-10
Office of Human Resources & Admin.
Director, RW-30
Office of Program Mgmt. & Integ.
Director, RW-40
Office of Waste Accept., Stor., & Tran.
Forrestal Building
Washington, DC 20585

Attn: Project Director
Yucca Mountain Site Characterization Office
Director, RW-3
Office of Quality Assurance
P.O. Box 30307
Las Vegas, NV 89036-0307

US Department of Energy
Albuquerque Operations Office
Attn: National Atomic Museum Library
P.O. Box 5400
Albuquerque, NM 87185-5400

US Department of Energy
Research & Waste Management Division
Attn: Director
P.O. Box E
Oak Ridge, TN 37831

US Department of Energy (5)
Carlsbad Area Office
Attn: G. Dials
D. Galbraith
M. McFadden
R. Lark
J. A. Mewhinney
P.O. Box 3090
Carlsbad, NM 88221-3090

US Department of Energy
Office of Environmental Restoration and
Waste Management
Attn: M Frei, EM-30
Forrestal Building
Washington, DC 20585-0002

US Department of Energy (3)
Office of Environmental Restoration and
Waste Management
Attn: J. Juri, EM-34, Trevion II
Washington, DC 20585-0002

US Department of Energy
Office of Environmental Restoration and
Waste Management
Attn: S. Schneider, EM-342, Trevion II
Washington, DC 20585-0002

US Department of Energy (2)
Office of Environment, Safety & Health
Attn: C. Borgstrom, EH-25
R. Pelletier, EH-231
Washington, DC 20585

US Department of Energy (2)
Idaho Operations Office
Fuel Processing & Waste Mgmt. Division
785 DOE Place
Idaho Falls, ID 83402

US Environmental Protection Agency (2)
Radiation Protection Programs
Attn: M. Oge
ANR-460
Washington, DC 20460

Boards

Defense Nuclear Facilities Safety Board
Attn: D. Winters
625 Indiana Ave. NW, Suite 700
Washington, DC 20004

Nuclear Waste Technical Review Board (2)
Attn: Chairman
J. L. Cohon
1100 Wilson Blvd., Suite 910
Arlington, VA 22209-2297

State Agencies

Attorney General of New Mexico
P.O. Drawer 1508
Santa Fe, NM 87504-1508

Environmental Evaluation Group (3)
Attn: Library
7007 Wyoming NE
Suite F-2
Albuquerque, NM 87109

NM Energy, Minerals, and Natural
Resources Department
Attn: Library
2040 S. Pacheco
Santa Fe, NM 87505

NM Environment Department (3)
Secretary of the Environment
Attn: Mark Weidler
1190 St. Francis Drive
Santa Fe, NM 87503-0968

NM Bureau of Mines & Mineral Resources
Socorro, NM 87801

Laboratories/Corporations

Battelle Pacific Northwest Laboratories
Battelle Blvd.
Richland, WA 99352

Los Alamos National Laboratory
Attn: B. Erdal, INC-12
P.O. Box 1663
Los Alamos, NM 87544

Tech Reps, Inc. (3)
Attn: J. Chapman (1)
Loretta Robledo (2)
5000 Marble NE, Suite 222
Albuquerque, NM 87110

Westinghouse Electric Corporation (5)
Attn: Library
J. Epstein
J. Lee
B. A. Howard
R. Kehrman
P.O. Box 2078
Carlsbad, NM 88221

S. Cohen & Associates
Attn: Bill Thurber
1355 Beverly Road
McLean, VA 22101

**National Academy of Sciences,
WIPP Panel**

Howard Adler
Oxyrase, Incorporated
7327 Oak Ridge Highway
Knoxville, TN 37931

Tom Kiess
Board of Radioactive Waste Management
GF456
2101 Constitution Ave.
Washington, DC 20418

Rodney C. Ewing
Department of Geology
University of New Mexico
Albuquerque, NM 87131

Charles Fairhurst
Department of Civil and Mineral Engineering
University of Minnesota
500 Pillsbury Dr. SE
Minneapolis, MN 55455-0220

B. John Garrick
PLG Incorporated
4590 MacArthur Blvd., Suite 400
Newport Beach, CA 92660-2027

Leonard F. Konikow
US Geological Survey
431 National Center
Reston, VA 22092

Carl A. Anderson, Director
Board of Radioactive Waste Management
National Research Council
HA 456
2101 Constitution Ave. NW
Washington, DC 20418

Christopher G. Whipple
ICF Kaiser Engineers
1800 Harrison St., 7th Floor
Oakland, CA 94612-3430

John O. Blomeke
720 Clubhouse Way
Knoxville, TN 37909

Sue B. Clark
University of Georgia
Savannah River Ecology Lab
P.O. Drawer E
Aiken, SC 29802

Konrad B. Krauskopf
Department of Geology
Stanford University
Stanford, CA 94305-2115

Della Roy
Pennsylvania State University
217 Materials Research Lab
Hastings Road
University Park, PA 16802

David A. Waite
CH_2 M Hill
P.O. Box 91500
Bellevue, WA 98009-2050

Thomas A. Zordon
Zordan Associates, Inc.
3807 Edinburg Drive
Murrysville, PA 15668

Universities

University of New Mexico
Geology Department
Attn: Library
141 Northrop Hall
Albuquerque, NM 87131

University of Washington
College of Ocean & Fishery Sciences
Attn: G. R. Heath
583 Henderson Hall, HN-15
Seattle, WA 98195

Libraries

Thomas Brannigan Library
Attn: D. Dresp
106 W. Hadley St.
Las Cruces, NM 88001

Government Publications Department
Zimmerman Library
University of New Mexico
Albuquerque, NM 87131

New Mexico Junior College
Pannell Library
Attn: R. Hill
Lovington Highway
Hobbs, NM 88240

New Mexico State Library
Attn: N. McCallan
325 Don Gaspar
Santa Fe, NM 87503

New Mexico Tech
Martin Speere Memorial Library
Campus Street
Socorro, NM 87810

WIPP Public Reading Room
Carlsbad Public Library
101 S. Halagueno St.
Carlsbad, NM 88220

Foreign Addresses

Atomic Energy of Canada, Ltd.
Whiteshell Laboratories
Attn: B. Goodwin
Pinawa, Manitoba, CANADA R0E 1L0

Francois Chenevier (2)
ANDRA
Route de Panorama Robert Schumann
B. P. 38
92266 Fontenay-aux-Roses, Cedex
FRANCE

Claude Sombret
Centre d'Etudes Nucleaires de la Vallee Rhone
CEN/VALRHO
S.D.H.A. B.P. 171
30205 Bagnols-Sur-Ceze
FRANCE

Commissariat a L'Energie Atomique
Attn: D. Alexandre
Centre d'Etudes de Cadarache
13108 Saint Paul Lez Durance Cedex
FRANCE

Bundesanstalt fur Geowissenschaften und
Rohstoffe
Attn: M. Langer
Postfach 510 153
D-30631 Hannover
GERMANY

Bundesministerium fur Forschung und
Technologie
Postfach 200 706
5300 Bonn 2
GERMANY

Institut fur Tieflagerung
Attn: K. Kuhn
Theodor-Heuss-Strasse 4
D-3300 Braunschweig
GERMANY

Gesellschaft fur Anlagen und Reaktorsicherheit
(GRS)
Attn: B. Baltes
Schwertnergasse 1
D-50667 Cologne
GERMANY

Shingo Tashiro
Japan Atomic Energy Research Institute
Tokai-Mura, Ibaraki-Ken, 319-11
JAPAN

Netherlands Energy Research Foundation ECN
Attn: J. Prij
3 Westerduinweg
P.O. Box 1
1755 ZG Petten
THE NETHERLANDS

Svensk Karnbransleforsorjning AB
Attn: F. Karlsson
Project KBS (Karnbranslesakerhet)
Box 5864
S-102 48 Stockholm
SWEDEN

Nationale Genossenschaft fur die Lagerung
Radioaktiver Abfalle (2)
Attn: S. Vomvoris
P. Zuidema
Hardstrasse 73
CH-5430 Wettingen
SWITZERLAND

AEA Technology
Attn: J. H. Rees
D5W/29 Culham Laboratory
Abington, Oxfordshire OX14 3DB
UNITED KINGDOM

AEA Technology
Attn: W. R. Rodwell
044/A31 Winfrith Technical Centre
Dorchester, Dorset DT2 8DH
UNITED KINGDOM

AEA Technology
Attn: J. E. Tinson
B4244 Harwell Laboratory
Didcot, Oxfordshire OX11 ORA
UNITED KINGDOM

Internal

MS	Org.	
1324	6115	P. B. Davies
1320	6831	E. J. Nowak
1322	6121	J. R. Tillerson
1328	6849	D. R. Anderson
1328	6848	H. N. Jow
1335	6801	M. Chu
1341	6832	J. T. Holmes
1395	6800	L. Shephard
1395	6821	M. Marietta
0443	9117	J. G. Arguello
0443	9117	C. M. Stone
0443	9117	A. Fossum
0443	9117	G. D. Sjaardema
0815	5932	F. T. Mendenhall
0425	5932	R. C. Lincoln
0716	6113	D. E. Munson
1341	6822	K. W. Larson
1395	6801	P. Swift
1341	6832	L. H. Brush
3128	6848	D. M. Stoelzel
1328	6849	P. Vaughn
1324	6115	A. R. Lappin
1324	6115	S. W. Webb
1345	6832	B. M. Butcher (5)
0841	9100	P. J. Hommert
0841	9101	T. C. Bickel
0443	9117	H. S. Morgan
1330	6811	K. Hart (2)
1330	4415	NWM Library (20)
9018	8940-2	Central Technical Files
0899	4916	Technical Library (5)
0619	12690	Review and Approval Desk (2), For DOE/OSTI